

ESTIMATING HEAT SOURCES AND FLUXES IN THERMALLY STRATIFIED CANOPY FLOWS USING HIGHER-ORDER CLOSURE MODELS

MARIO SIQUEIRA^{1,2*} and GABRIEL KATUL^{1,2}

¹*Nicholas School of the Environment and Earth Sciences, Duke University, Durham, Box 90328, North Carolina 27708-0328, U.S.A.;* ²*Civil and Environmental Engineering, Duke University, Durham, North Carolina, U.S.A.*

(Received in final form 17 September 2001)

Abstract. Over the past two decades, several inverse methods have been proposed to estimate scalar source and sink strengths from measured mean concentration profiles within the canopy volume (hereafter termed the 'inverse' problem). These inverse methods commonly assumed neutral atmospheric stability conditions for the entire canopy volume. For non-neutral conditions, atmospheric stability corrections in inverse schemes were limited to adjusting the integral time scale or other flow statistics to match well-established surface-layer similarity relations above the canopy. Such stability corrections do not explicitly consider the local stability effects within the canopy volume. Currently, there is no satisfactory inverse scheme that explicitly accounts for local atmospheric stability for canopy turbulence. A Eulerian inverse method that explicitly accounts for local atmospheric stability within the canopy is developed using second-order closure principles. Field testing the method is conducted using temperature measurements from two field experiments collected in an even-aged uniform loblolly pine forest. It is demonstrated that by accounting for local atmospheric stability in the inversion scheme, the agreement between modelled sensible heat flux calculations and measurements improve by 60% for stable conditions, 10% for near-neutral conditions and 20% for unstable conditions

Keywords: Canopy scalar source/sink, Canopy scalar transport, Inverse problem, Stability effects.

1. Introduction

Estimating scalar source and sink (S_c) distribution and vertical fluxes (F_c) within and above forested canopies continues to be a critical research problem in biosphere-atmosphere exchange processes and plant ecology (Wofsy et al., 1993; Gao et al., 1993; Vermetten et al., 1994; Baldocchi and Harley, 1995; Culf et al., 1997; Baldocchi and Meyers, 1998; Simpson et al., 1998; Lee, 1998; Rannik, 1998; Malhi et al., 1998; Potosnak et al., 1999; Gu et al., 1999; Anthoni et al., 1999; Law et al., 1999). For many scalars, it is impractical to measure the vertical distribution of S_c within the canopy beyond the leaf scale (e.g. using porometry). On the other hand, mean scalar concentration (\bar{c}) profiles are often readily measured within the canopy volume. Since sources and fluxes are directly related by a scalar concen-

* E-mail: mbs4@duke.edu



tration budget equation, the problem is reduced to inferring S_c from the readily measured \bar{c} . This problem is commonly termed the ‘inverse problem’ (Raupach, 1988, 1989a,b) and is the subject of the present investigation.

Attempts to estimate scalar flux distribution inside canopies goes back to the early 1960s (Begg et al., 1964; Wright and Brow, 1964; Brow and Covey, 1966). These studies made use of first-order closure models or (K-theory) in order to calculate a single diffusivity coefficient from measurements and estimations of the energy budget components. With a modelled diffusivity, they inferred the source/sink and flux distribution. It is now recognized that K-theory is not suitable for source/sink calculation within a canopy because of its inability to reproduce countergradient fluxes, a well-known phenomenon for canopy turbulence.

Over the past two decades, two basic approaches emerged to estimate S_c from \bar{c} without resorting to K-theory: Lagrangian dispersion models (e.g., the localized near field theory of Raupach (1989a) and the more recent analytical model of Warland and Thurtell (2000)), and higher-order Eulerian closure models. Both approaches were successfully used to infer S_c and F_c from measured \bar{c} in several field and laboratory experiments (Raupach et al., 1992; Denmead and Raupach, 1993; Denmead, 1995; Katul et al., 1997a, 2001; Massman and Weil, 1999; Katul and Albertson, 1999; Leuning, 2000; Denmead et al., 2000; Siqueira et al., 2000; Warland and Thurtell, 2000).

All inverse methods up to now assume that scalar transport within the canopy volume is neutral (Katul et al., 2001). Leclerc et al (1987) suggests that stability inside the canopy, which could differ from above the canopy, cannot be determined through corrections to boundary conditions only. Recent studies by Leuning (2000) and Siqueira et al. (2000) demonstrate the important role of local stability effects within the canopy volume for vegetation types ranging from an irrigated rice canopy to a pine forest. The next logical step in inverse modelling is to develop new methods that can explicitly account for local atmospheric stability inside the canopy. The objective then is to develop and test a second-order closure inverse model that accounts for local buoyancy effects on scalar transport within the canopy volume when estimating S_c from \bar{c} . The proposed inverse method builds on an earlier approach by Katul and Albertson (1999) to include local thermal stratification in the flux-budget equations. The proposed method, described next, is tested using two heat dispersion experiments in a Loblolly pine stand at Duke Forest near Durham, North Carolina.

2. Experiment

2.1. STUDY SITE

Two sets of experiments were conducted at the Blackwood Division of the Duke Forest near Durham, North Carolina (36°02'N, 79°8'W, elevation 163 m) in the U.S.A. The first set comprises a heat dispersion experiment aimed at assessing

how well the model recovers vertical source and flux distribution within the canopy when atmospheric stability is included. The second set is a long-term heat dispersion experiment aimed at assessing how well the model recovers temporal patterns of sensible heat flux above the canopy for a wide range of non-neutral atmospheric stability conditions.

Both experiments were conducted in a uniformly planted loblolly pine (*Pinus taeda* L.) forest stand, extending 300–600 m in the east-west direction and 1000 m in the north-south direction. The mean canopy height, h , was 14.0 m (± 0.5 m) in 1998. Topographic variations within the stand were small (terrain slope changes $< 5\%$) such that the influence of topography on the turbulent fluxes can be neglected (Kaimal and Finnigan, 1994).

2.2. THE HEAT DISPERSION EXPERIMENT

To assess the vertical distribution of scalar fluxes inside the canopy, simultaneous mean temperature profiles and turbulence statistics were measured. The mean temperature was collected at 8 levels (1.5 m, 3.5 m, 5.5 m, 7.5 m, 9.5 m, 11.5 m, 13.5 m and 15.5 m) using shielded copper constantan thermocouples (20 gauge, diameter = 0.812 mm). For this field setup, the thermocouples were sampled every 1 second and averaged every 30 minutes. The thermocouples were calibrated in a water bath prior to the experiment such that the maximum differences between them did not exceed 0.1 °C. The water bath calibration spanned a temperature range from 5 °C to 40 °C.

The velocity statistics and turbulent heat flux distribution were simultaneously measured at 3.0 m, 4.9 m, 8.6 m, 10.9 m, 12.2 m, and 15.5 m above the forest floor using six Campbell Scientific triaxial sonic anemometers (CSAT3, Campbell Scientific, Logan, UT, U.S.A.). The sampling frequency was 10 Hz and the sampling period was also 30 minutes per run. The experimental setup is detailed in Siqueira et al. (2000). More than 150 runs were collected in year 2000 over two periods: April 19 to 23 and October 20 to 27, and for a wide range of stability conditions. The stability regime above the canopy was determined using the stability parameter $\zeta = -(z - d)/L$, where d is the zero-plane displacement (determined from the centroid of the momentum sink profile), L is the Obukhov length determined from the friction velocity (u_*) and sensible heat flux (H) measured above the canopy. Neutral conditions were assumed when $|\zeta| < 0.05$.

2.3. THE LONG-TERM HEAT DISPERSION EXPERIMENT

To assess the applicability of the proposed method to long-term fluxes above the canopy, a long-term record of sensible heat fluxes above the canopy and mean temperature profiles within the canopy were used. This data set is being collected as part of an ongoing long-term CO₂ flux monitoring initiative at the Duke AmeriFlux site (Katul et al., 1999; Lai et al., 2000).

The sensible heat fluxes above the canopy were measured using an eddy-covariance system comprising of a Campbell Scientific triaxial sonic anemometer. The CSAT3 was positioned at 15.5 m above the forest floor, and was anchored on a horizontal bar extending 1.5 m away from the top of the walkup tower.

The analog signals from these instruments were sampled at 5 Hz using a Campbell Scientific 21X data logger with all digitized signals transferred to a computer via an optically isolated RS232 interface for future processing. All the 5-Hz raw measurements processing was performed using the procedures described in Katul et al. (1997a, b).

The shoot silhouette area index, a value analogous to the leaf area index (LAI), was measured in the vertical direction at increments of 1 m by a pair of Licor LAI 2000 plant canopy analyzers four times a year starting in 1996. A subset of this data set was used to compute the velocity statistics. For modelling the flow statistics within the canopy, it was assumed that the LAI 2000 plant canopy analyzer measurements are analogous to the leaf area density $a(z)$.

3. Theory

In this section, the Eulerian inverse model for canopy heat transport is presented. Measured mean temperature gradients were used as the primary model input.

3.1. SCALAR TRANSPORT IN THE EULERIAN FRAME OF REFERENCE

Applying time and horizontal averaging, the steady state scalar conservation equation for planar homogeneous high Reynolds and Peclet numbers flow (neglecting molecular diffusion) can be written as (Finnigan, 1985; Raupach, 1988):

$$\frac{\partial \langle \bar{T} \rangle}{\partial t} = 0 = -\frac{\partial \langle \overline{w'T'} \rangle}{\partial z} + S_T. \quad (1)$$

The overbar and $\langle \cdot \rangle$ denote time and horizontal averaging respectively (Raupach and Shaw, 1982) and primes denote fluctuations from time averages; T is the air temperature, w is the vertical velocity, $\langle \overline{w'T'} \rangle = F_T$ is the vertical kinematic turbulent flux of sensible heat, and S_T is the heat source and sink.

The corresponding time and horizontally averaged conservation equation for $\langle \overline{w'T'} \rangle$ as a function of $\langle \bar{T} \rangle$ is:

$$\frac{\partial \langle \overline{w'T'} \rangle}{\partial t} = 0 = -\langle \overline{w^2} \rangle \frac{\partial \langle \bar{T} \rangle}{\partial z} - \frac{\partial \langle \overline{w'w'T'} \rangle}{\partial z} - \frac{1}{\rho} \left\langle \overline{T' \frac{\partial p'}{\partial z}} \right\rangle + \frac{g}{\langle \bar{T} \rangle} \langle \overline{T_V'^2} \rangle, \quad (2)$$

where ρ is air density. In (2), scalar drag and waving source production were neglected. The four terms on the right-hand-side of (2) represent respectively the

production of turbulent flux due to interactions between turbulence and mean temperature gradient (production term), transport of the turbulent flux (transport term), destruction by pressure-temperature interaction (dissipation term), and buoyant production. In fact, the buoyancy production term is a function of virtual temperature. However, here we only consider its dependence on actual temperature, a simplification that decouples sensible and latent heat allowing solution for sensible heat flux alone, which is the scope of the study. Furthermore the optimization of closure constants partially corrects for the simplification.

3.2. CLOSURE APPROXIMATIONS

The transport and dissipation terms on the right-hand-side of (2) are unknowns requiring closure approximations or additional budgets. In this study, the transport term derived by Meyers and Paw U (1987) and the dissipation term modelled after Finnigan (1985) were adopted. These approximations are:

$$\langle \overline{w'w'T'} \rangle = \frac{\tau}{C_8} \left[-\langle \overline{w'w'w'} \rangle \frac{\partial \langle \bar{T} \rangle}{\partial z} - \langle \overline{w'T'} \rangle \frac{\partial \langle \overline{w'w'} \rangle}{\partial z} - 2\langle \overline{w'w'} \rangle \frac{\partial \langle \overline{w'T'} \rangle}{\partial z} \right] \quad (3)$$

$$\left\langle \overline{T' \frac{\partial p'}{\partial z}} \right\rangle = C_4 \frac{\langle \overline{w'T'} \rangle}{\tau} - \frac{1}{3} \frac{g}{\langle \bar{T} \rangle} \langle \overline{T'^2} \rangle. \quad (4)$$

In (3) and (4), C_4 and C_8 are closure constants and τ is an Eulerian relaxation time scale given by

$$\tau = \frac{q^2}{\langle \epsilon \rangle}, \quad (5)$$

where q ($= \sqrt{\langle u_i' u_i' \rangle}$) is a characteristic turbulent velocity, $\langle \epsilon \rangle$ is the mean rate of viscous dissipation, and u_i are the velocity components in the x_1 (or x), x_2 (or y), and x_3 (or z) directions, respectively, with x_1 aligned along the mean wind direction so that $\overline{u_2} = 0$.

Finally, to estimate $\langle \overline{T'^2} \rangle$, the temperature variance budget is considered:

$$\frac{\partial \langle \overline{T'^2} \rangle}{\partial t} = 0 = -2\langle \overline{w'T'} \rangle \frac{\partial \langle \bar{T} \rangle}{\partial z} - \frac{\partial \langle \overline{w'T'T'} \rangle}{\partial z} - 2\langle \epsilon_{TT} \rangle, \quad (6)$$

with the following closure models for the transport term $\langle \overline{w'T'T'} \rangle$ and the dissipation term $\langle \epsilon_{TT} \rangle$,

$$\langle \overline{w'T'T'} \rangle = \frac{\tau}{C_8} \left[-2\langle \overline{w'w'T'} \rangle - \overline{w'^2} \frac{\partial \langle \overline{T'^2} \rangle}{\partial t} - 2\langle \overline{w'T'} \rangle \frac{\partial \langle \overline{w'T'} \rangle}{\partial z} \right], \quad (7)$$

$$\langle \epsilon_{TT} \rangle = C_5 \frac{\overline{\langle T'^2 \rangle}}{\tau}, \quad (8)$$

where C_5 is a closure constant.

Upon combining (2) to (8), a set of second-order ordinary differential equations (ODEs) can be derived for estimating $\overline{\langle w'T' \rangle}$ and $\overline{\langle T'^2 \rangle}$, but only if the flow statistics $\overline{\langle w'^2 \rangle}$ and $\overline{\langle w'^3 \rangle}$, τ (measured or modelled), and temperature gradient, which can be estimated from measured profiles, are known. The boundary conditions proposed by Katul and Albertson (1999) and Meyers and Paw U (1987) were adopted for Equations (2) and (6) respectively. The closure constants were optimized for best statistics in $\overline{\langle w'T' \rangle}$ and the numeric values used were $C_4 = 2.5$, $C_8 = 3.0$ and $C_5 = 0.5$, which are within the range reported in the literature (Meyers and Paw U, 1987; Katul and Albertson, 1999; Siqueira et al., 2000; Katul et al., 2001). For the purpose of this study, the second-order closure model of Wilson and Shaw (1977) was used to estimate these variables. For completeness, the basic closure equations are listed in Appendix A.

4. Results and Discussion

The inverse model calculations modified to include atmospheric stability were compared to eddy-covariance sensible heat flux measurements. For reference, the same comparisons were repeated but with atmospheric stability corrections neglected. First, the vertical heat dispersion experiment is considered in order to assess the ability of the model to reproduce the vertical attenuation of heat fluxes within the canopy. Departures between model results and measurements are also discussed in the context of the closure approximations used. Next, the applicability of such inverse calculations to long-term estimation of $\overline{\langle w'T' \rangle}$ is considered. However, prior to presenting these comparisons, the generation of the flow statistics is discussed. Comparisons with velocity measurements inside the canopy are also presented.

4.1. GENERATION OF THE FLOW STATISTICS

Using the measured leaf area density and the drag coefficient estimated by Katul and Chang (1999), the second-order closure model of Wilson and Shaw (1977) was used to generate the flow statistics inside the canopy. Here, we focus on two variables required for scalar transport calculations: σ_w and $\overline{\langle w'^3 \rangle}$. Figure 1 demonstrates that the second-order closure model of Wilson and Shaw (1977) can reasonably reproduce the measured σ_w ($= \sqrt{\overline{\langle w'^2 \rangle}}$) and $\overline{\langle w'^3 \rangle}$, at least for the purposes of scalar transport.

In these calculations, the effects of local thermal stability on the velocity statistics were neglected for simplicity. In order to evaluate if such a simplification is

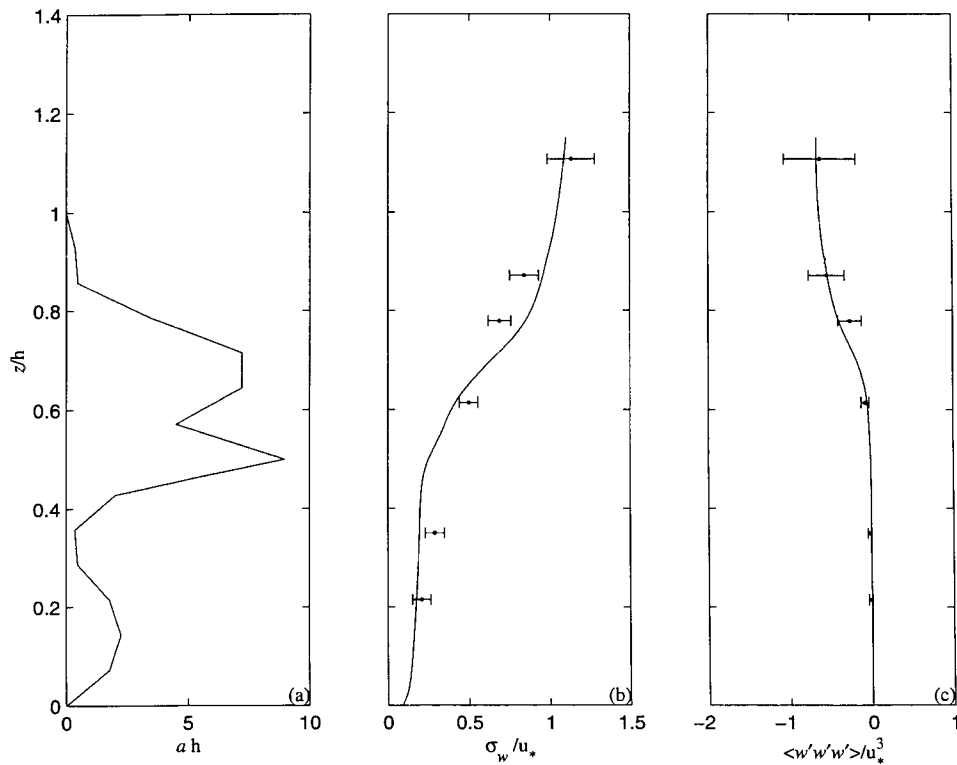


Figure 1. Panel (a) leaf area density interpolated from 14 measurements. Panels (b) and (c) comparison between measured (dots) and modelled (solid line) ensemble velocity statistics for normalized vertical velocity standard deviation and normalized vertical velocity skewness, respectively. Error bars represent one standard deviation.

reasonable, the ensemble-averaged normalized production terms of turbulent kinetic energy (TKE) are compared in Figure 2 for the three stability conditions. The measured streamwise velocity, shear stresses and heat fluxes were used to calculate the shear and buoyant production terms (Kaimal and Finnigan, 1994, p. 86). The wake production is computed from the Wilson and Shaw (1977) model formulation but using the measured streamwise velocity.

It is evident from Figure 2 that the buoyancy term in the TKE budget is at least one order of magnitude smaller than one of the other two production terms over most of the flow domain. Wake production appears dominant inside the canopy while the shear production is dominant above it. This demonstrates that the added complexity in including local buoyancy effects on the velocity statistics need not translate into increased model skill. Similar conclusions were also presented in Hsieh et al. (Hsieh, C. I., Siqueira, M., Katul, G. and Chu, C. R.: 2001, 'Predicting Scalar Source-Sink and Flux Distributions within a Forest Canopy Using a Lagrangian Stochastic Dispersion Model', submitted to: *Boundary-Layer Meteorol.*) for the same forest stand. In the latter study, they compared the results of an inverse

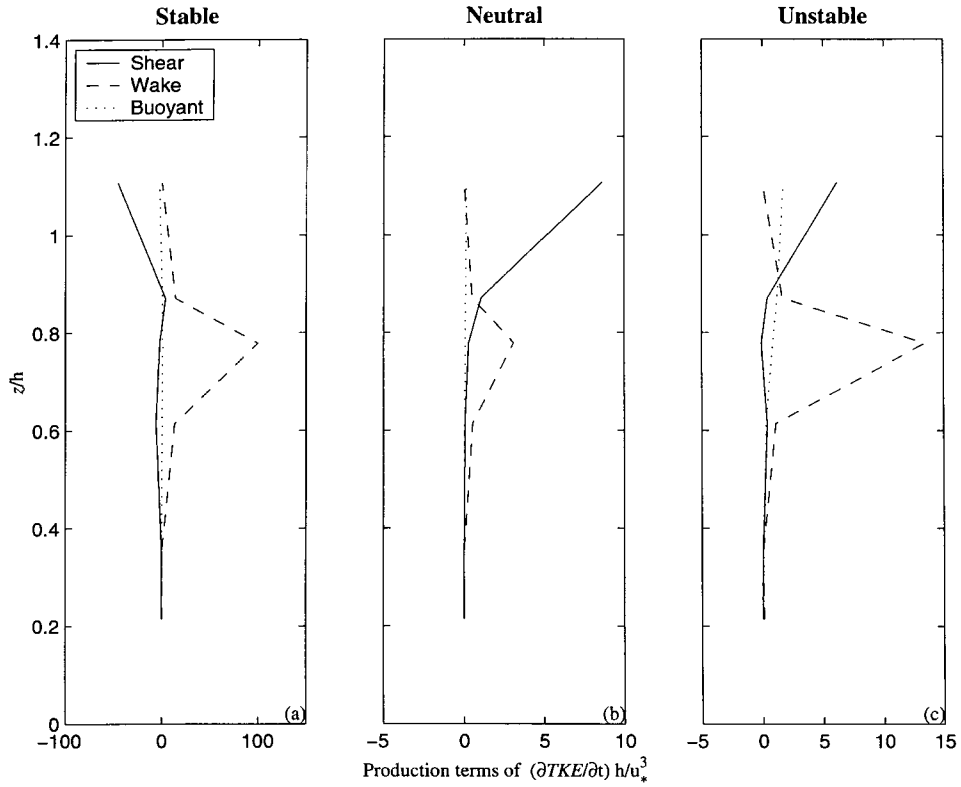


Figure 2. Comparison between ensemble averaged normalized production terms of turbulent kinetic energy (TKE): Shear production (solid line), wake production (dashed line), and buoyant production (dotted line) for three stability classes: Panel (a) stable stability condition; panel (b) neutral stability condition; and panel (c) unstable stability condition.

model driven by measured run-to-run velocity statistics profiles, in which buoyancy effects on the velocity statistics would be resolved, and ensemble averaged profiles, in which the buoyancy effects would be averaged out. They found no significant differences in the modelled scalar source distribution.

4.2. VERTICAL HEAT DISPERSION RESULTS

Measured and modelled $\langle w'T' \rangle$ at all six levels are compared in Figure 3 for three stability classes: stable, neutral, and unstable atmospheric conditions. For reference, the model results when neglecting the $\langle T'^2 \rangle$ correction to the $\langle w'T' \rangle$ budget are displayed. Figure 3 also includes the results of a method that will be further discussed in Section 4.3. Table I presents the overall regression results for such comparisons and for the different stability classes. It is evident that root-mean squared errors (RMSE) are significantly reduced when $\langle T'^2 \rangle$ corrections are applied, particularly for stable conditions.

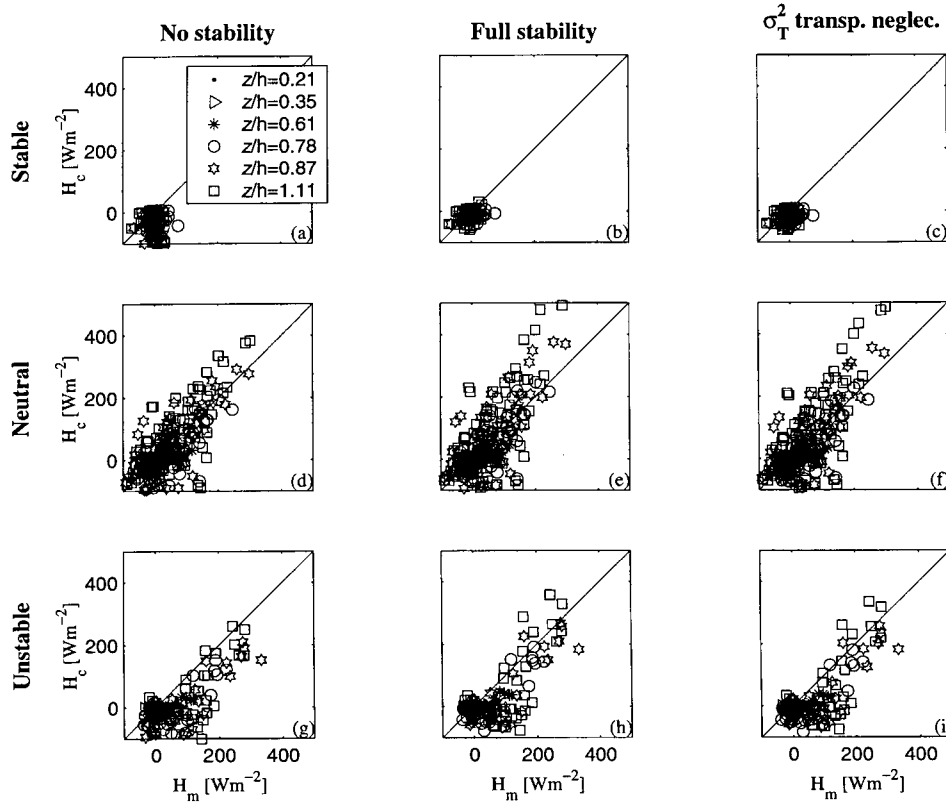


Figure 3. The 1-to-1 comparisons between measured (x-axis) and modelled (y-axis) heat flux. Panel rows are for the three stability conditions: Top row, (a), (b) and (c), under stable stability condition; middle row, (d), (e) and (f) under neutral stability condition; and bottom row, (g), (h) and (i), under unstable stability condition. Panel columns are for different calculation procedures: Left column, (a), (d) and (g), for calculation without the inclusion of the temperature variance budget; middle column, (b), (e) and (h), calculation including the full temperature variance budget; and right column (c), (f) and (i) calculation including the simplified temperature variance budget (neglecting the temperature variance transport term). Different symbols stand for different heights above the forest floor.

To further investigate the role of local stability on the inversion scheme, a comparison between the measured and modelled $\overline{\langle w'T' \rangle}$ vertical attenuation within the canopy volume is presented in Figure 4 for the three stability classes. The $\overline{\langle T'^2 \rangle}$ corrections on the normalized $\overline{\langle w'T' \rangle}$ attenuation are most pronounced for unstable conditions. This is further investigated in Figure 5, which shows the modelled components of the $\overline{\langle w'T' \rangle}$ budget for the three stability classes. From Figure 5, the modelled contribution of the buoyancy term relative to other production terms is most significant for unstable conditions.

Given that $\overline{\langle T'^2 \rangle}$ corrections significantly contribute to the $\overline{\langle w'T' \rangle}$ budget (and hence inverse model calculations), it is logical to consider whether the attenuation of $\overline{\langle T'^2 \rangle}$ is also reproduced by the closure model calculations. In Figure 6, the

TABLE I

Comparison between measured and modelled sensible heat flux for the three calculation procedures and the three stability conditions.

		No stability	Full stability	σ_T^2 transp. neglec.
Stable	N	228	228	228
	Slope	0.11	0.24	0.18
	Intercept [W m^{-2}]	-25.40	-7.11	-10.60
	RMSE [W m^{-2}]	47.80	19.20	22.70
	R	0.05	0.30	0.20
Neutral	N	480	480	480
	Slope	0.91	1.06	1.01
	Intercept [W m^{-2}]	-8.97	-0.71	-2.63
	RMSE [W m^{-2}]	56.90	57.20	54.60
	R	0.70	0.75	0.75
Unstable	N	222	222	222
	Slope	0.54	0.70	0.66
	Intercept [W m^{-2}]	-23.70	-14.60	-15.90
	RMSE [W m^{-2}]	74.10	61.80	62.20
	R	0.65	0.73	0.73

The regression model is of the form $y = Ax + B$, where y is the modelled heat flux and x is the measured heat flux. In the table N stands for the number of runs under each stability condition, the RMSE and the correlation coefficient R are also shown.

measured and modelled $\overline{\langle T'^2 \rangle}$ attenuations for the three stability classes are compared. It was found that the closure model ‘over-attenuated’ $\overline{\langle T'^2 \rangle}$, which could be a consequence of the optimization of constants done for $\overline{\langle w'T' \rangle}$ and not for $\overline{\langle T'^2 \rangle}$, especially C_5 . Yet, despite this ‘over-attenuation’, it is clear that the inclusion of $\overline{\langle T'^2 \rangle}$ improves the local estimation of $\overline{\langle w'T' \rangle}$ within the canopy (e.g., Table I). The errors in $\overline{\langle T'^2 \rangle}$ are more pronounced in the deeper layers in the canopy where the heat flux is small, attenuating their impact.

One complication to the routine application of this approach is that the solution to Equations (2)–(6) along with their closure approximations requires an iterative approach not free from numerical convergence difficulties. This added complexity in the numerical solution motivated the evaluation of an alternative and parsimonious approach that retains much of the $\overline{\langle T'^2 \rangle}$ effects on $\overline{\langle w'T' \rangle}$ but does not require an iterative approach.

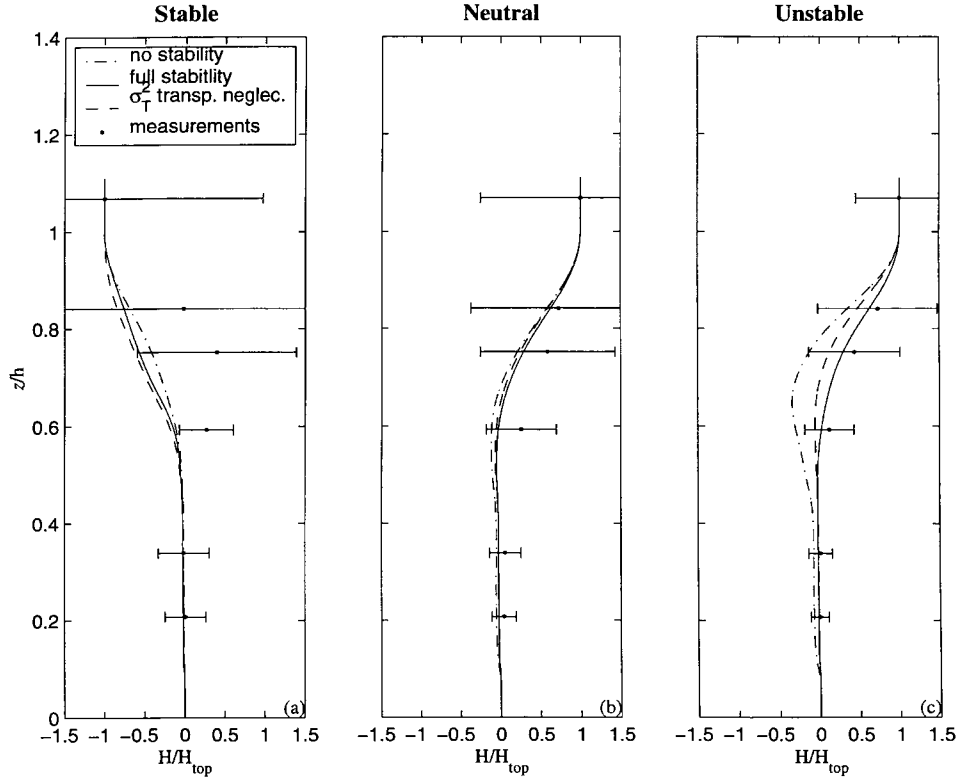


Figure 4. Comparison between ensemble measured (dots) and calculated (lines) heat flux attenuation profile for the three stability conditions: Panel (a) stable condition; panel (b) neutral condition, and panel (c) unstable condition. Different lines stands for different calculation procedures labelled in Figure 3.

4.3. PRACTICAL SIMPLIFICATIONS

From the previous analysis, the agreement between measured and modelled $\langle \overline{w'T'} \rangle$ is improved by considering $\langle \overline{T'^2} \rangle$ despite the fact that the model does not adequately reproduce the measured $\langle \overline{T'^2} \rangle$. This agreement suggests that a simplified budget for $\langle \overline{T'^2} \rangle$, of the form

$$\langle \overline{T'^2} \rangle = -\frac{\tau \langle \overline{w'T'} \rangle}{C_5} \frac{\partial \langle \overline{T} \rangle}{\partial z}, \quad (9)$$

may prove to be sufficiently adequate for sensible heat source and flux inferences. That is, neglecting the flux-transport term in the temperature variance budget may still permit an explicit estimation of $\langle \overline{T'^2} \rangle$ without resorting to an iterative proced-

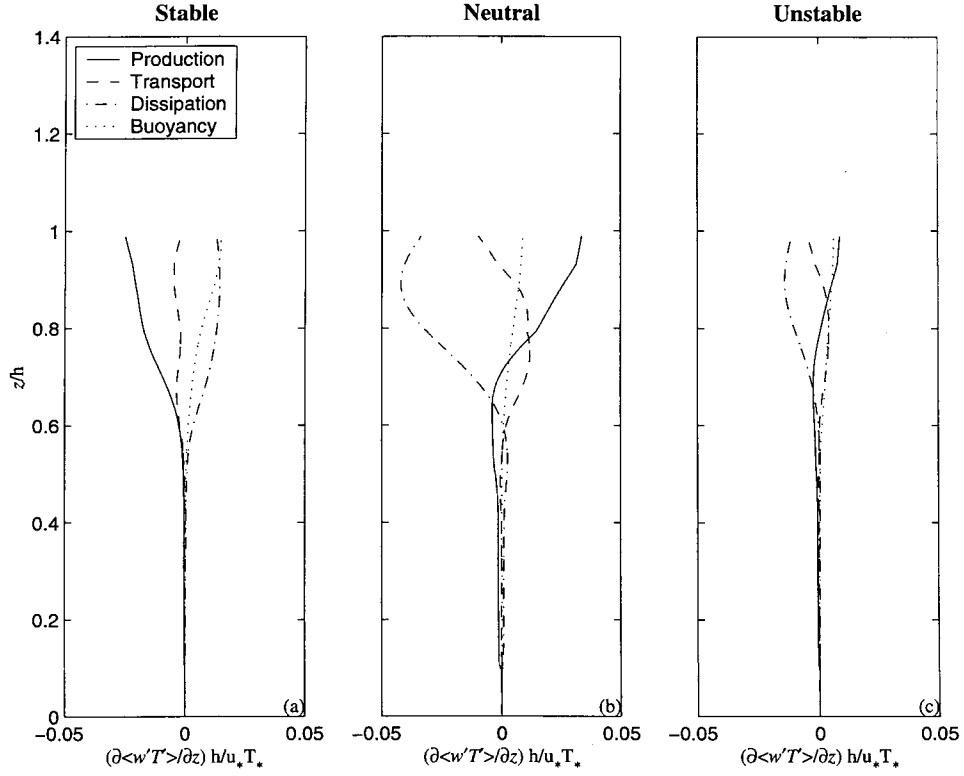


Figure 5. Comparison between the normalized components of the heat flux budget equation for the three stability classes. Solid line is the shear production term, dashed line is the turbulent transport term, dot-dashed line is the dissipation term, and dotted line is for buoyant production term. Panel (a) stable stability condition, panel (b) neutral stability condition and (c) unstable stability condition.

ure. Upon combining Equations (2) to (5) with (9) the method reduces in solving one single ordinary differential equation for $\langle w'T' \rangle$:

$$A_1(z) \frac{d^2 \langle w'T' \rangle}{dz^2} + A_2(z) \frac{d \langle w'T' \rangle}{dz} + A_3(z) \langle w'T' \rangle = A_4(z), \quad (10)$$

where the coefficients A_1 , A_2 , A_3 and A_4 are given by

$$A_1(z) = \frac{2\tau}{C_8} \langle \overline{w'w'} \rangle,$$

$$A_2(z) = \frac{\tau}{C_8} \frac{d \langle \overline{w'w'} \rangle}{dz} + 2 \frac{d}{dz} \left(\frac{\tau}{C_8} \langle \overline{w'w'} \rangle \right),$$

$$A_3(z) = \frac{d}{dz} \left(\frac{\tau}{C_8} \frac{d \langle \overline{w'w'} \rangle}{dz} \right) - C_4 \frac{1}{\tau} - \frac{4}{3} \frac{g}{\langle \bar{T} \rangle} \frac{\tau}{C_5} \frac{d \langle \bar{T} \rangle}{dz},$$

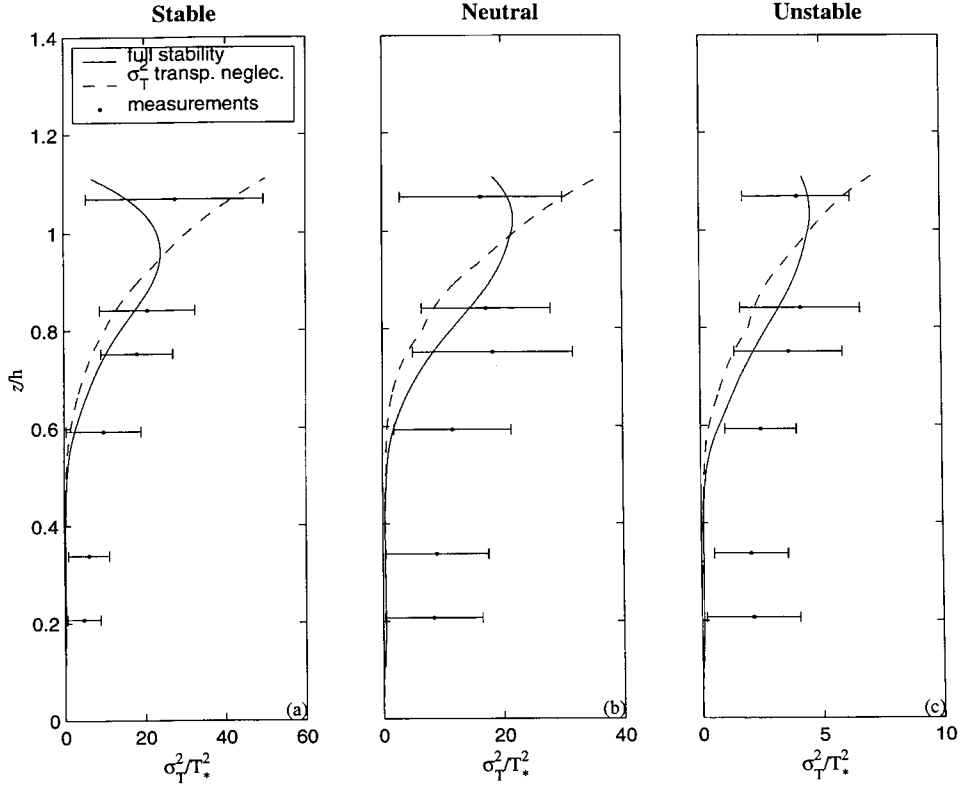


Figure 6. Comparison between ensemble measured (dots) and calculated (lines) temperature variance attenuation profile for the three stability conditions: Panel (a) stable condition; Panel (b) neutral condition, and panel (c) unstable condition. Different lines are for different calculation procedures labelled in Figure 3.

$$A_4(z) = \overline{w'w'} \frac{d\langle \bar{T} \rangle}{dz} - \frac{d}{dz} \left(\frac{\tau}{C_8} \overline{w'w'w'} \right) \frac{d\langle \bar{T} \rangle}{dz} - \left(\frac{\tau}{C_8} \overline{w'w'w'} \right) \frac{d^2\langle \bar{T} \rangle}{dz^2}.$$

All the calculations shown in Figures 3, 4, and 6 were repeated and it was found that indeed the flux comparisons between the two models are comparable (see, e.g., Figures 3 and 4). As expected, the agreement between measured and modelled was substantially reduced (Figure 6). Interestingly, the degree of degradation in modelled $\langle \bar{T}^2 \rangle$ did not linearly translate into comparable degradation in modelled $\overline{w'T'}$ (see Table I), again suggesting some robustness in the simplified scheme.

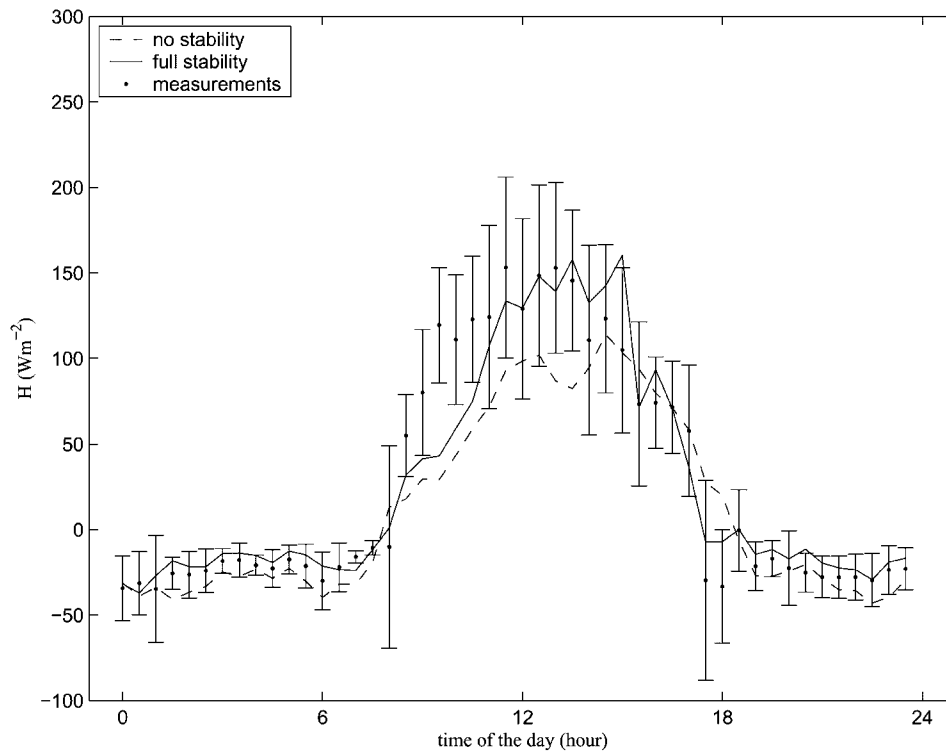


Figure 7. Time variation of the time ensemble averaged heat flux at the canopy top measured (dots) and calculated (lines). Solid line is for the heat flux calculated including the temperature variance budget equation and dashed line without temperature variance budget.

4.4. LONG-TERM APPLICABILITY

To illustrate the applicability of this method for long-term data sets, we estimated the sensible heat flux at the canopy top for a period of seven months with and without a $\overline{\langle T'^2 \rangle}$ correction. The comparison between measured and modelled heat flux, bin-averaged by time of day, is shown in Figure 7. During the nighttime period, the inclusion of stability effects decreased the negative heat flux, which was overestimated due to the very high temperature gradient inside the canopy. For the transition periods, where conditions are mostly near-neutral (but unsteady), the improvement is marginal, as expected. During the daylight period, when unstable conditions prevail, a much better agreement is obtained when $\overline{\langle T'^2 \rangle}$ is included in the calculation.

All in all it is clear that accounting for $\overline{\langle T'^2 \rangle}$ (vis-à-vis setting $\overline{\langle T'^2 \rangle} = 0$) improves the comparison between modelled and measured $\overline{\langle w'T' \rangle}$ by about 30% for this forest stand.

5. Conclusions

An inverse method that explicitly accounts for local atmospheric stability effects within the canopy using Eulerian second-order closure principles has been developed. The proposed method was tested using temperature measurements from two field experiments collected in an even-aged uniform pine forest. This study demonstrated the following:

- The influence of atmospheric stability is primarily on the scalar-temperature covariance. In contrast, the local stability effects on the local velocity statistics such as variances are not as pronounced.
- By accounting for atmospheric stability via $\overline{\langle T'^2 \rangle}$, the ability to infer the $\overline{\langle w'T' \rangle}$ distribution within and above the canopy for stable, unstable, and near-neutral conditions improved.
- A simplified version of this inversion scheme that models $\overline{\langle T'^2 \rangle}$ via a balance between production and dissipation reproduced $\overline{\langle w'T' \rangle}$ variations within the canopy volume reasonably well.
- The proposed method is sufficiently robust for use in long-term flux monitoring initiatives.

Acknowledgements

The authors would like to thank Chun-Ta Lai and Karen Wesson for their help in setting up the multilevel field experiment. The first author also thanks the ‘Conselho Nacional de Desenvolvimento Científico e Tecnológico (CNPq)’ of Brazil for their support. Additional support was provided by the National Science Foundation (NSF-EAR), the Department of Energy (DOE) through the FACE-FACTS project and through the National Institute of Global Environmental Change (NIGEC) through the Southeast Regional Center at the University of Alabama, Tuscaloosa (DOE cooperative agreement DE-FC030-90ER61010). Finally, we thank Judd Edburn and the Duke Forest staff for their overall assistance during many of these field experiments and also Prof. Cheng-I Hsieh for his helpful comments.

Appendix A: Wilson and Shaw’s (1977) Model

Upon time and horizontally averaging the mean momentum and Reynolds stress equations for neutral conditions, the second-order closure model of Wilson and Shaw (1977) reduces to

$$0 = -\frac{d\overline{\langle u'w' \rangle}}{dz} - C_d a(z) \langle \bar{u} \rangle^2,$$

$$\begin{aligned}
0 &= -\overline{\langle w'^2 \rangle} \frac{d\langle \bar{u} \rangle}{dz} + 2 \frac{d}{dz} \left(q \lambda_1 \frac{d\langle \overline{u'w'} \rangle}{dz} \right) - \frac{q \langle \overline{u'w'} \rangle}{3 \lambda_2} + C_w q^2 \frac{d\langle \bar{u} \rangle}{dz}, \\
0 &= -2 \langle \overline{u'w'} \rangle \frac{d\langle \bar{u} \rangle}{dz} + \frac{d}{dz} \left(q \lambda_1 \frac{d\langle \overline{u'^2} \rangle}{dz} \right) + 2 C_d a(z) \langle \bar{u} \rangle^3 \\
&\quad - \frac{q}{3 \lambda_2} \left(\langle \overline{u'^2} \rangle - \frac{q^2}{3} \right) - \frac{2 q^3}{3 \lambda_3}, \\
0 &= \frac{d}{dz} \left(q \lambda_1 \frac{d\langle \overline{v'^2} \rangle}{dz} \right) - \frac{q}{3 \lambda_2} \left(\langle \overline{v'^2} \rangle - \frac{q^2}{3} \right) - \frac{2 q^3}{3 \lambda_3}, \\
0 &= \frac{d}{dz} \left(3 q \lambda_1 \frac{d\langle \overline{w'^2} \rangle}{dz} \right) - \frac{q}{3 \lambda_2} \left(\langle \overline{w'^2} \rangle - \frac{q^2}{3} \right) - \frac{2 q^3}{3 \lambda_3}.
\end{aligned} \tag{A1}$$

In Equation (A1), u_i ($u_1 = u$, $u_2 = v$, $u_3 = w$) are the instantaneous velocity components along x_i , x_i ($x_1 = x$, $x_2 = y$, $x_3 = z$) are the longitudinal, lateral, and vertical directions, respectively, λ_1 , λ_2 , and λ_3 are characteristic length scales for the triple-velocity correlation, the pressure-velocity gradient correlation, and viscous dissipation, respectively, C_w is a constant, C_d is the foliage drag coefficient and $a(z)$ is the leaf area density.

With estimates of the characteristics length scales λ_1 , λ_2 , and λ_3 , and the constant C_w the five ordinary differential equations in (A.1) can be solved for the five flow variables $\langle \bar{u} \rangle$, $\langle \overline{u'w'} \rangle$, $\langle \overline{u'^2} \rangle$, $\langle \overline{v'^2} \rangle$, and $\langle \overline{w'^2} \rangle$, if appropriate boundary conditions are specified. The following neutral boundary conditions were used here: at $z/h = 1.1$, $\frac{\langle \bar{u} \rangle}{u_*} = 5.5$, $\frac{\sigma_u}{u_*} = 2.4$, $\frac{\sigma_v}{u_*} = 1.95$, $\frac{\sigma_w}{u_*} = 1.1$, $\frac{\langle \overline{uw} \rangle}{u_*^2} = -1.0$, and at $z/h = 0$, $\frac{\langle \bar{u} \rangle}{u_*} = 0$, $\frac{\sigma_w}{u_*} = 0$, $\frac{\sigma_v}{u_*} = 0$, $\frac{\sigma_u}{u_*} = 0$, $\frac{\langle \overline{uw} \rangle}{u_*^2} = 0$.

While more complex second-order closure schemes (e.g., Wilson, 1988) and third-order closure schemes have been developed for vegetation flow, recent studies by Katul and Albertson (1998) and Katul and Chang (1999) suggest that the Wilson and Shaw (1977) model performance is comparable to Wilson's (1988) and another third-order closure model for this pine forest.

References

- Anthoni, P. M., Law, B. E., and Unsworth, M. H.: 1999, 'Carbon and Water Vapor Exchange of an Open-Canopied Ponderosa Pine Ecosystem', *Agric. For. Meteorol.* **95**, 151–168.
- Baldocchi, D. and Harley, P. C.: 1995, 'Scaling Carbon Dioxide and Water Vapor Exchange from Leaf to Canopy in a Deciduous Forest. II Model Testing and Application', *Plant Cell Environ.* **18**, 1157–1173.
- Baldocchi, D. and Meyers, T.: 1998, 'On the Eco-Physiological and Biogeochemical Theory to Evaluate Carbon Dioxide, Water Vapor and Trace Gas Fluxes over Vegetation: A Perspective', *Agric. For. Meteorol.* **90**, 1–25.

- Begg, J. E., Bierhuizen, J. F., Lemon, E. R., Misra, D. K., Slatyer, R. O., and Stern, W. R.: 1964, 'Diurnal Energy and Water Exchanges in Bulrush Millet in a Area of High Solar Radiation', *Agric. Meteorol.* **1**, 294–312.
- Brown, K. W. and Covey, W.: 1966, 'The Energy-Budget Evaluation of the Micro-Meteorological Transfer Processes within a Cornfield', *Agric. Meteorol.* **3**, 73–96.
- Culf, A. D., Fisch, G., Malhi, Y., and Nobre, C. A.: 1997, 'The Influence of the Atmospheric Boundary Layer on Carbon Dioxide Concentrations over a Tropical Forest', *Agric. For. Meteorol.* **85**, 149–158.
- Denmead, O. T.: 1995, 'Novel Meteorological Methods for Measuring Trace Gas Fluxes', *Phil. Trans. Roy. Soc. of London A* **351**, 383–396.
- Denmead, O. T. and Raupach, M. R.: 1993, 'Methods for Measuring Atmospheric Gas Transport in Agricultural and Forest System, in J. M. Duxbury, L. A. Harper, A. R. Mosier, and D. E. Rolston (eds.), *Agricultural Ecosystem Effects on Trace Gases and Global Climate Change*, American Society of Agronomy, Madison, pp. 19–43.
- Denmead, O. T., Harper, L. A., and Sharpe, R. R.: 2000, 'Identifying Sources and Sinks of Scalars in a Corn Canopy with Inverse Lagrangian Dispersion Analysis: I. Heat', *Agric. For. Meteorol.* **104**, 67–73.
- Finnigan, J. J.: 1985, 'Turbulent Transport in Plant Canopies', in B. A. Hutchinson and B. B. Hicks (eds.), *The Forest-Atmosphere Interactions*, D. Reidel, Norwell, MA, pp. 443–480.
- Gao, W., Wesely, M. L., and Doskey, P. V.: 1993, 'Numerical Modelling of the Turbulent Diffusion and Chemistry of NO_x, O₃, Isoprene, and Other Reactive Trace Gases in and above a Forest Canopy', *J. Geophys. Res.* **98**, 18,339–18,353.
- Gu, L. H., Shugart, H. H., Fuentes, J. D., Black, T. A., and Shewchuk, S. R.: 1999, 'Micro-meteorology, Biophysical Exchange and NEE Decomposition in a Two-Story Boreal Forest – Development and Test of an Integrated Model', *Agric. For. Meteorol.* **94**, 123–148.
- Kaimal, J. C. and Finnigan, J. J.: 1994, *Atmospheric Boundary Layer Flows: Their Structure and Measurement*, Oxford Press, 289 pp.
- Katul, G. G. and Albertson, J. D.: 1998, 'An Investigation of Higher Order Closure Models for a Forested Canopy', *Boundary-Layer Meteorol.* **89**, 47–74.
- Katul, G. G. and Albertson, J. D.: 1999, 'Modeling CO₂ Sources, Sinks and Fluxes within a Forest Canopy', *J. Geophys. Res.* **104**, 6081–6091.
- Katul, G. G. and Chang, W.-H.: 1999, 'Principal Length Scales in Second-Order Closure Models for Canopy Turbulence', *J. Appl. Meteorol.* **38**, 1631–1643.
- Katul, G. G., Hsieh, C. I., Bowling, D., Clark, K., Shurpali, N., Turnipseed, A., Albertson, J. D., Tu, K., Hollinger, D., Evans, B., Offerle, B., Anderson, D., Ellsworth, D., Vogel, C., and Oren, R.: 1999, 'Spatial Variability of Turbulent Fluxes in the Roughness Sublayer of an Even-Aged Pine Forest', *Boundary-Layer Meteorol.* **93**, 1–28.
- Katul, G. G., Leuning, R., Kim, J., Denmead, O. T., Miyata, A., and Harazono, Y.: 2001, 'Estimating CO₂ Source/Sink Distributions within a Rice Canopy Using Higher-Order Closure Models', *Boundary-Layer Meteorol.* **98**, 103–125.
- Katul, G. G., Oren, R., Ellsworth, D., Hsieh, C. I., Phillips, N., and Lewin, K.: 1997a, 'A Lagrangian Dispersion Model for Predicting CO₂ Sources, Sinks, and Fluxes in a Uniform Loblolly Pine (*Pinus taeda* L.) Stand', *J. Geophys. Res.* **102**, 9309–9321.
- Katul, G. G., Hsieh, C. I., Kuhn, G., Ellsworth, D., and Nie, D.: 1997b, 'Turbulent Eddy Motion at the Forest-Atmosphere Interface', *J. Geophys. Res.* **102**, 13,409–13,421.
- Lai, C. T., Katul, G., Oren, R., Ellsworth, D., and Schafer, K.: 2000, 'Modelling CO₂ and Water Vapor Turbulent Flux Distributions within a Forest Canopy', *J. Geophys. Res.* **105**, 26,333–26,351.
- Law, B. E., Baldocchi, D. D., and Anthoni, P. M.: 1999, 'Below-Canopy and Soil CO₂ Fluxes in a Ponderosa Pine Forest', *Agric. For. Meteorol.* **94**, 171–188.

- Leclerc, M. Y., Thurtell, G. W., and Kidd, G. E.: 1988, 'Measurements and Langevin Simulations of Mean Tracer Concentration Fields Downwind from a Circular Line Source inside an Alfalfa Canopy', *Boundary-Layer Meteorol.* **43**, 287–308.
- Lee, X. H.: 1998, 'On Micrometeorological Observations of the Surface-Air Exchange over Tall Vegetation', *Agric. For. Meteorol.* **91**, 39–49.
- Leuning, R.: 2000, 'Estimation of Scalar Source/Sink Distributions in Plant Canopies Using Lagrangian Dispersion Analysis: Corrections for Atmospheric Stability and Comparison with a Multilayer Canopy Model', *Boundary-Layer Meteorol.* **96**, 293–314.
- Malhi, Y., Nobre, A. D., Grace, J. G., Kruijt, B., Pereira, M. G. P., Culf, A., and Scott, S.: 1998, 'Carbon Dioxide Transfer over a Central Amazonian Rain Forest', *J. Geophys. Res.* **103**, 31,593–31,612.
- Massman, W. J. and Weil, J. C.: 1999, 'An Analytical One Dimensional Second-Order Closure Model of Turbulence Statistics and the Lagrangian Time Scale within and above Plant Canopies of Arbitrary Structure', *Boundary-Layer Meteorol.* **91**, 81–107.
- Meyers, T. and Paw U, K. T.: 1987, 'Modelling the Plant Canopy Micrometeorology with Higher-Order Closure Principles', *Agric. For. Meteorol.* **41**, 143–163.
- Potosnak, M., Wofsy, S. C., Denning, A. S., Conway, T. J., Munger, J. W., and Barnes, D. H.: 1999, 'Influence of Biotic Exchange and Combustion Sources on Atmospheric CO₂ Concentrations in New England from Observations at a Forest Flux Tower', *J. Geophys. Res.* **104**, 9561–9569.
- Rannik, U.: 1998, 'On the Surface Similarity at a Complex Forest Site', *J. Geophys. Res.* **103**, 8685–8697.
- Raupach, M. R.: 1989a, 'Applying Lagrangian Fluid Mechanics to Infer Scalar Source Distributions from Concentration Profiles in Plant Canopies', *Agric. For. Meteorol.* **47**, 85–108.
- Raupach, M. R.: 1989b, 'A Practical Lagrangian Method for Relating Scalar Concentrations to Source Distributions in Vegetation Canopies', *Quart. J. Roy. Meteorol. Soc.* **115**, 609–632.
- Raupach, M. R.: 1988, 'Canopy Transport Processes, in W. L. Steffen and O. T. Denmead (eds.), *Flow and Transport in the Natural Environment*, Springer-Verlag, New York, pp. 95–127.
- Raupach, M. R. and Shaw, R. H.: 1982, 'Averaging Procedures for Flow within Vegetation Canopies', *Boundary-Layer Meteorol.* **22**, 79–90.
- Raupach, M. R., Denmead, O. T., and Dunin, F. X.: 1992, 'Challenges in Linking Atmospheric CO₂ Concentrations to Fluxes at Local and Regional Scales', *Aust. J. Bot.* **40**, 697–716.
- Simpson, I. J., Thurtell, G. W., Neumann, H. H., Den Hartog, G., and Edwards, G. C.: 1998, 'The Validity of Similarity Theory in the Roughness Sublayer above Forest', *Boundary-Layer Meteorol.* **87**, 69–99.
- Siqueira, M., Lai, C. T., and Katul, G.: 2000, 'Estimating Scalar Sources, Sinks, and Fluxes in a Forest Canopy Using Lagrangian, Eulerian, and Hybrid Inverse Models', *J. Geophys. Res.* **105**, 29,475–29,488.
- Vermetten, A. W. M., Ganzeveld, L., Jeuken, A., Hofschreuder, P., and Mohren, G. M. J.: 1994, 'CO₂ Uptake by a Stand of Douglas-Fir – Flux Measurements Compared with Model-Calculations', *Agric. For. Meteorol.* **72**, 57–80.
- Warland, J. S. and Thurtell, G. W.: 2000, 'A Lagrangian Solution to the Relationship between a Distributed Source and Concentration Profile', *Boundary-Layer Meteorol.* **96**, 453–471.
- Wilson, J. D.: 1988, 'A Second Order Closure Model for Flow through Vegetation', *Boundary-Layer Meteorol.* **42**, 371–392.
- Wilson, N. R. and Shaw, R. H.: 1977, 'A Higher Order Closure Model for Canopy Flow', *J. Appl. Meteorol.* **16**, 1198–1205.
- Wofsy, S. C., Goulden, M. L., Munger, J. W., Fan, S. M., Bakwin, P. S., Daube, B. C., Bassow, S. L., and Bazzaz, F. A.: 1993, 'Net Exchange of CO₂ in a Mid-Latitude Forest', *Science* **260**, 1314–1317.
- Wright J. L. and Brown, K. W.: 1967, 'Comparison of Momentum and Energy Balance Methods of Computing Vertical Transfer within a Crop', *Agron. J.* **59**, 427–432.